

# The Impact of Lead Geometry and Discrete Doping on NWFET Operation

S. Berrada, N. Cavassilas, L. Raymond, M. Lannoo and M. Bescond

IM2NP, UMR CNRS 7334, Bât. IRPHE, Technopôle de Château-Gombert, 13384 Marseille, cedex 13, France  
e-mail: salim.berrada@im2np.fr

Si nanowire MOSFET (NWFET) is one of the most promising device to reach the end of the technological roadmap. However due to the continuous reduction of the channel length, resistance of access regions may appear as the main contributor of the global resistance [1]. A physically consistent modeling of nanowire transistors then requires a realistic description of the open character of the system *via* access regions. The aim of this work is to emphasize the importance of considering both realistic lead geometry and discrete doping. We use a 3D real-space non-equilibrium Green's function (NEGF) approach where electron-phonon scattering is treated within the self-consistent Born approximation (SCBA) [2].

We consider two lead geometries for NWFETs with  $L_G=8$  nm as schematically shown in Fig. 1. We shall refer to the device with the uniform transverse section in Fig. (1.a) by (UN), and by (NUN) to its nonuniform counterpart (Fig. (1.b)). We first assumed for both devices a continuous dopant concentration of  $10^{20}\text{cm}^{-3}$  in the source (S), drain (D) and access regions (AR) - represented by yellow regions in Fig. 1.  $I_D-V_{GS}$  curves show that both devices exhibit the same threshold voltages  $V_{th}$ , subthreshold slopes and ON state currents (Fig.2). This result is in accordance with the results previously obtained for double-gate devices [3].

However, a concentration of  $10^{20}\text{cm}^{-3}$  corresponds on average to less than two dopants in a volume of  $2\times 2\times 4\text{ nm}^{-3}$ . As a result, the commonly accepted assumption of continuous doping in the access regions is no longer justified.

As a sound example we replace the continuous doping of the AR in both UN and NUN devices by one dopant exactly localized on the same positions along the channel symmetry axis (Fig. 3).  $I_D-V_{GS}$

curves (Fig. 4) show that subthreshold behavior has not been affected by the discrete aspect of the doping in AR. This result is in line with the fact that subthreshold behavior is mainly controlled by the channel characteristics, which remained unchanged in both devices.

However, as expected [4], the discrete dopants degrade the on-current. Surprisingly, the degradation depends on the access region geometry since current reductions are 19 and 30% respectively for the UN and NUN at  $V_{GS}=0.49$  V.

To understand the higher degradation in the NUN device, let's analyze the LDOS at this bias for both transistors. In the UN device (Fig. 5), we can clearly distinguish the two impurity levels (IL) localized around the impurity positions. Moreover, the IL are close to the Fermi level ( $E_F$ ) of their respective contacts and are strongly coupled to S and D, thus contributing efficiently to the injection and extraction of carriers in the device. In NUN device, the IL is no longer a quasi-localized state of the coulombic potential (Fig. 6). Indeed the larger cross-section reduces the impurity binding energy [5], leading to delocalized IL's well above the Fermi levels of the contacts, reducing the injection efficiency and resulting in a reduction of the ON current.

This result shows the importance of considering both realistic lead geometry and discreteness of the dopants to provide an accurate modeling of NWFETs, where access regions will have an increasing influence.

## REFERENCES

- [1] Y. He *et al.*, *Appl. Phys. Lett.* **105**, 213502 (2014).
- [2] H. Carrillo-Nunez *et al.*, *J. Appl. Phys.* **116**, 164505 (2014).
- [3] R. Venugopal *et al.*, *J. Appl. Phys.* **95**, 292 (2004).
- [4] A. Asenov *et al.*, *IEEE-Trans. Elec. Dev.* **61**, 2745 (2014).
- [5] M. Diarra *et al.*, *Phys. Rev. B* **75**, 045301 (2007).

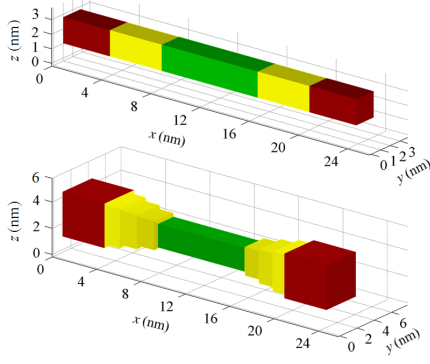


Fig. 1. Considered gate-all-around NWFETs (a) UN : with uniform cross-section of  $2 \times 2 \text{ nm}^2$  and (b) NUN : non uniform cross section. Same channel length  $L_{CH}=8 \text{ nm}$  and cross-section of  $2 \times 2 \text{ nm}^2$  (green) are assumed for both devices. Gate insulator is  $1 \text{ nm}$  thick. Source and drain are represented in red and are  $4 \text{ nm}$  long, while the access regions are represented in yellow (with a length of  $4 \text{ nm}$ ). Source (drain) cross-section in NUN device is  $3.6 \times 3.6 \text{ nm}^2$ . For all the simulations  $V_{DS}=0.3 \text{ V}$  and  $T=300 \text{ K}$ .

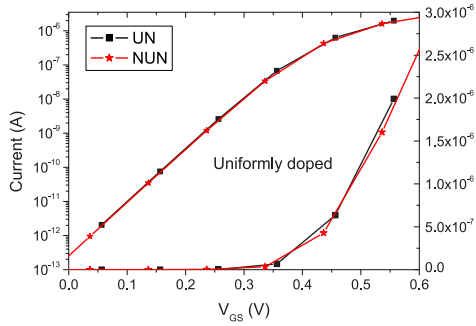


Fig. 2.  $I_D - V_{GS}$  with uniformly doped access regions for UN (squares) and for NUN (stars) devices.

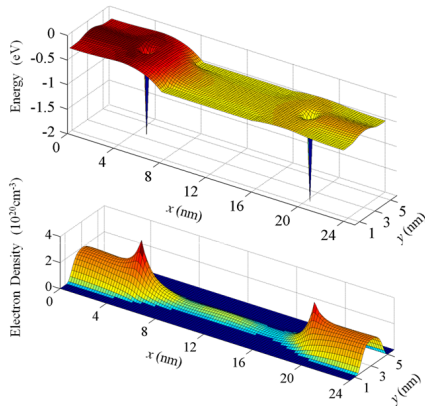


Fig. 3. (a) Conduction band along transport axis located at  $z=2.8 \text{ nm}$  (middle of the device) of the NUN device with impurities placed in AR at  $x = 5 \text{ nm}$  and  $x=19 \text{ nm}$ . (b) corresponding electron density.  $V_{GS}=0.49 \text{ V}$ .

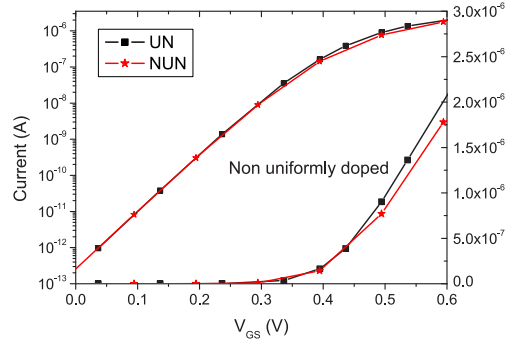


Fig. 4. Figure 4 :  $I_D - V_{GS}$  with impurities placed in AR along the channel symmetry axis at  $x = 5 \text{ nm}$  and  $x=19 \text{ nm}$  for UN device (squares) and NUN device (stars). The curves have been shifted to provide the same  $V_{th}$ .

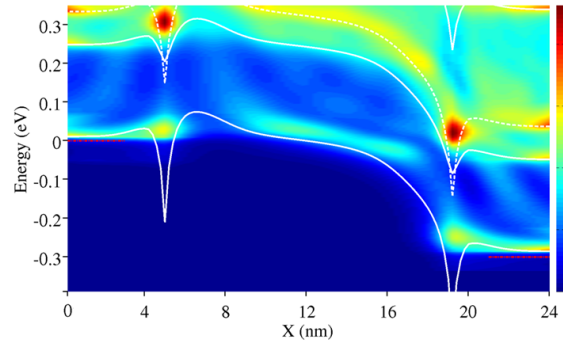


Fig. 5. LDOS at  $V_{GS}=0.49 \text{ V}$  for the UN device with impurities placed in AR along the channel symmetry axis at  $x = 5 \text{ nm}$  and  $x=19 \text{ nm}$ . White lines corresponds to the eigenvalues of transverse valleys ( $m_t$  in the transport direction) and white dashed lines correspond to the two others. Fermi levels in source and drain are indicated with red dashed lines.

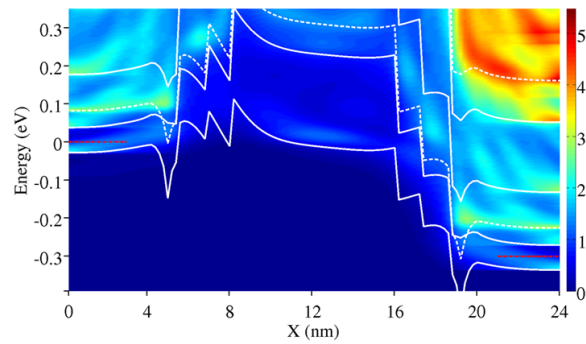


Fig. 6. Similar physical quantities as in Fig. 5 but for the NUN device.